Journal of Molecular Liquids 300 (2020) 112368

Contents lists available at ScienceDirect

Journal of Molecular Liquids

journal homepage: www.elsevier.com/locate/molliq

# Novel ruthenium doped $TiO_2$/reduced graphene oxide hybrid as highly selective sensor for the determination of ambroxol

Shikandar D. Bukkitgar [a], Nagaraj P. Shetti [a,*], Ramesh S. Malladi [b], Kakarla Raghava Reddy [c,*], Shankara S. Kalanur [d], Tejraj M. Aminabhavi [e]

[a] Center for Electrochemical Science and Materials, Department of Chemistry, K.L.E Institute of Technology, Gokul, Hubballi-580030, Karnataka, India
[b] Department of Chemistry, BLDEA's V. P. Dr. P.G. Halakatti College of Engineering and Technology, Vijayapur-586103, Karnakata, India
[c] School of Chemical and Biomolecular Engineering, The University of Sydney, Sydney, NSW 2006, Australia
[d] Department of Material Science and Engineering, School of Engineering, Ajou University, Suwon 443-739, Republic of Korea
[e] Department of Pharmaceutics, Soniya College of Pharmacy, Dharwad 580 002, Karnataka, India

ARTICLE INFO

*Article history:*
Received 19 November 2019
Received in revised form 14 December 2019
Accepted 20 December 2019
Available online 23 December 2019

*Keywords:*
Doped $TiO_2$ nanoparticles
Graphene oxide
Modified electrodes
Electrochemical sensor
Cyclic voltammetry
Aambroxol
Healthcare

ABSTRACT

Clinical trials and quality control processes are always in need of an effective sensor for the trace level estimation of analyte. In present work, a sensor for ambroxol drug at electrochemically reduced graphene oxide (ErGO) and ruthenium doped $TiO_2$ nanoparticles (RT) is proposed. RT/ErGO/CPE hybrid showed an increase in the peak current up to five-folds, signifying the potential of the sensor when compared with the nascent carbon paste electrode. The previously established calibration graph was used and LOD and LOQ in the range 0.1 μM–0.6 μM was 1.0 nM and 4.0 nM, respectively. The effect on peak current and potential was studied at different scan rates, pH and concentration. Repeatability of the sensor was confirmed by inter and intraday investigations of the ambroxol drug. The selectivity of the sensor was studied in the presence of common excipients. Further, the method was used successfully for the determination of ambroxol in pharmaceutical dosage forms as well as in human urine samples.



## 1. Introduction

Respiratory diseases such as cystic fibrosis (CF), chronic obstructive pulmonary disease (COPD), bronchiectasis, chronic bronchitis, and asthma, are indicated by hypersecretion of airway mucus. These respiratory diseases have led to excessive usage and development drugs affecting mucus secretion: mucoactive agents [1]. These drugs have the ability to alter the production of mucus, its composition, and mucociliary epithelium interaction. They are classified on supposed mechanisms of action such as mucokinetics, mucolytics, mucoregulators, and expectorants [2]. Ambroxol (ABX) is gifted with properties to stimulate effect on mucociliary clearance and belongs to 8th active metabolite of bromhexine. It is been effectively used to assess its effect in COPD and in preventing chronic bronchitis [3–5]. Further, reports of ABX use include controlling CF, post chest operations to prevent complications such as bronchopulmonary, in newborns to prevent hyaline membrane disease and as antioxidant therapy [6–9]. Past reports have outlined distinct methods for ABX determination in biological and pharmaceutical samples using high-performance liquid chromatography [10–12], UV-spectrophotometry [13], gas chromatography [14], voltammetry [15] and chromatography with amperometric detection [16]. However, the availability of only a few automated procedures, which are expensive, contain solutions and are time-consuming, given the scope of development of new analytical methods with improved performance.

Voltammetric methods based on electrochemical sensors have advantages such as they are less expensive, simple, and accurate with high sensitivity and selectivity. In continuation of our ongoing program of research, we focused here on the development of electrochemical sensors for investigation of the biologically active molecules [17–21] involving the fabrication of electrode material either by chemical or surface modification with nanoparticles. In the earlier literature, investigations on ABX describing its voltammetric behavior and quantification using a glassy carbon electrode with a differential pulse voltammetric technique have been made [15]. Experiments were

* Corresponding authors.
*E-mail addresses:* dr.npshetti@gmail.com (N.P. Shetti), reddy.chem@gmail.com (K.R. Reddy).

https://doi.org/10.1016/j.molliq.2019.112368
0167-7322/

performed in 0.2 M $H_2SO_4$ with oxidation peak corresponding to ABX at 1.05 V and detection limit was $9.4 \times 10^{-7}$ M in the linear range of $6.0 \times 10^{-6}$–$6.0 \times 10^{-5}$ M. In other investigations, carbon film resistor electrodes were used to propose a flow injection amperometric method for the determination of ABX in 0.1 M $H_2SO_4$ [22] with the limit of detection of $7.61 \times 10^{-8}$. However, these proposed methods might result in reduced sensitivity to estimate ABX because of electrostatic repulsions between the protonated form of ABX in highly acidic medium and the surface of the working electrode having a positive potential.

In electrochemical research, carbon paste and glassy carbon electrodes are quite crucial as they are cheap to fabricate and can be alternative to metal electrodes [23–25]. The carbon fiber microelectrodes could enhance the electrochemical investigation of biological samples [26]. In recent years, graphene, and carbon nanotubes have revolutionized the fields of applied electrochemistry. Graphene (GR), an allotrope of carbon, has flat monolayer carbon atoms in $sp_2$-hybridized form arranged in a honeycomb structure and the material has gained much attention due to it varied properties such as high modulus, high thermal conductivity [27,28], high surface area [29], optical transparency [30], and electrical conductivity [31]. These properties have prompted their applications as supercapacitors, batteries, solar cells, transistors, and sensors [32].

The use of oxide semiconductors such as ZnO [33,34], $In_2O_3$ [35], $SnO_2$ [36] and $TiO_2$ [37,38] have been helpful to increase the bandgap and hence, these materials have the unique place in electronics area due to their versatile properties. Among the various semiconductors used, $TiO_2$ nanoparticles, in view of their wide bandgap, stability, enhanced catalytic activity, high surface area, as well as low toxicity have been widely used as catalysts [39]. However, $TiO_2$ can be made more effective by doping with other metal ions, which would alter the physicochemical properties. For instance, ruthenium as a dopant in $TiO_2$ nanocrystals has been widely employed [40,41]. Ruthenium-doped $TiO_2$ (RT) with a high electron affinity has shown excellent photocatalytic ability [42]. Additional advantages are offered by doping Ru ions into $TiO_2$, resulting in an increased life of the charge carriers [43]. Thus, it was felt that RT can be a promising material for the fabrication of electrode with high sensitivity and selectivity.

In this research, for the first time, we propose an easy method to fabricate a highly efficient novel electrochemical sensor comprising electrochemically reduced graphene oxide loaded with ruthenium-doped $TiO_2$ nanoparticles. Investigations were concerned with peak potential and current obtained for the oxidation of ABX by varying the parameters such as pH, temperature, scan rate, and concentration in order to evaluate the kinetic parameters. Additionally, SWV method with a lower detection limit compared to other methods reported for the trace level detection of ABX in pharmaceutical and human urine samples. Recovery studies were also performed, which suggest its potential as a sensor for the detection of ABX.

## 2. Experimental

### 2.1. Materials and reagents

Graphene oxide, sodium dodecyl sulfate and ambroxol received from Sigma-Aldrich were used unchanged. The investigations were performed in between 3.0 and 11.2 pH, prepared using $H_3PO_4$, $KH_2PO_4$, $Na_3PO_4$, and $Na_2HPO_4$ from sd Fine-Chem Ltd. Mumbai, India [44]. For interference study lactose, urea, gum acacia, oxalic acid and glycine from the Himedia Laboratories Pvt. Ltd. Mumbai, India were used.

### 2.2. Apparatus

The voltammetric investigation was performed using the electrochemical analyzer. Experiments were carried in 10 mL single cell containing appropriate ABX and a buffer solution whose pH was adjusted using Elico pH meter. Conventional three electrodes system i.e., Modified CPE, Ag/AgCl and platinum wire (working, reference and counter electrode respectively) were dipped in the cell containing analyte solution and the voltammograms were recorded using a personal computer with software CHI version 12.16.

### 2.3. Sample preparation

Ten ambroxol tablets (Ambrolite 30 mg) purchased in a local pharmacy were finely powdered in a mortar. The powdered tablet was dissolved in water to prepare 1.0 mM of the solution in a volumetric flask. Taking suitable aliquots from the stock solutions, appropriate solutions were prepared by dissolving in a phosphate buffer of pH 6.0 [45,46]. The analysis was performed by the standard addition method using a square wave voltammetric technique operated at 0.4 to 1.3 V after the accumulation time of 45 s. Further, the recovery was determined to investigate the applicability of the proposed sensor in a pharmaceutical dosage form prepared for the estimation.

### 2.4. Carbon paste electrode (CPE) preparation

7.0 g of graphite powder was weighed accurately and mixed with 3.0 g of paraffin oil to prepare CPE. A portion of the resulting paste after complete homogenization for 30 min was filled in a PTFE tube with an inserted copper wire for establishing the electrical contact. The surface was slowly and carefully smoothened on a sandpaper. The resulting electrode is the CPE, which was scanned in phosphate buffer solution (pH 6.0) in the potential range 0.0–1.2 V at the scan rate 0.1 V/s for 10 cycles to get a stable voltammogram. This has helped to activate the surface of CPE [47].

### 2.5. Preparation of electrochemically reduced graphene oxide (ErGO) modified electrode

Graphite powder, graphene oxide and paraffin oil were mixed in the ratio 7:3:2 and firmly filled in a PTFE tube. The surface was smoothened and the resulting electrode was used as a graphene oxide-modified electrode (GO/CPE). Further, the electrochemical reduction of graphene oxide was carried out to obtain rGO modified electrode. For this, a similar composition of electrode as above for GO/CPE was dipped in a cell containing 0.1 M (pH = 12.0) KOH solution along with a counter and a reference electrode. The surface was scanned in the potential window −1.2 to 0.0 V for 20 cycles with 0.1 V/s as a scan rate. The surface was further cleaned with distilled water and used for further analysis, resulting in the electrochemical reduction of graphene oxide designated as ErGO/CPE. For each reading, a new paste was used and the process continued as before.

### 2.6. Preparation of RT/ErGO/CPE

Ru-doped $TiO_2$ (RT) nanoparticles were prepared as similar to the previous report [48]. 1.0 mg of RT nanoparticles were suspended in 1.0 mL acetone, and mixed by sonication for 15 min. The resultant suspension was drop-casted onto the surface of ErGO/CPE and was dried. The electrode obtained was referred to as RT/ErGO/CPE.

## 3. Results and discussion

### 3.1. Electrochemical reduction of GO

Reducing GO electrochemical is a promising method for the conversion of GO to form rGO, which avoids the use of hazardous chemicals such as hydrazine and also the burden of byproduct disposal. The electrochemical reduction was performed by producing a graphene oxide thin film on the surface of glass, plastic or metal electrode by using cyclic or linear pulse voltammetric technique in sodium phosphate buffer

solution between −1.0 and 1.0 potential window previously. The reduction peak was observed at −0.7 V.

The reduction of GO was performed by mixing GO with CPE and recording the cyclic voltammograms (Fig. 1). The voltammogram recorded with KOH as the electrolyte solution affirmed the reduction of GO with peaks observed at −0.7 V. and the process was by the electron transfer from a graphitic sheet of carbon paste to the GO forming ErGO. Successive cycling reduced the peak current for the reduction of GO suggesting the sluggish electron transport and saturation of the electrode surface. Thus fabricated electrode surface was considered to be the ErGO/CPE.

### 3.2. Voltammetric behavior of ABX

Voltammetric investigations of 0.1 mm ABX at CPE, RT/CPE, ErGO/CPE, and RT/ErGO/CPE surface (Fig. 2A) were performed using cyclic voltammetry. The voltammogram suggests that ABX is electrochemically active at 0.82 V. CPE with the least peak current showed two peaks, but these peaks were broader due to sluggish electron transfer. The modification of the electrode surface produced a single peak and no peak observed in the reverse scan direction suggested the electrode process to be irreversible. A comparison of voltammograms suggested that maximum peak current for ABX oxidation was for RT/ErGO/CPE. The effect of ErGO as an electrode modifier can be observed by comparing the voltammograms of CPE with ErGO/CPE. It was observed that the peak current for ErGO/CPE was two-timed higher than that of CPE due to the excellent electrocatalytic activity of rGO. The rGO has a high surface area, which enabled the increased surface loading of ABX, excellent electrochemical conductivity, and a small bandgap, which might have improved the conducting electrons between the ABX and the surface of the electrode. In addition, for nascent CPE, a sluggish electron transfer might have hindered the sensitivity, such that the observed peak current was quite low. Further, investigations were carried out for RT/ErGO/CPE at 0.1 mM of ABX at pH 6.0. Peak current for the nascent CPE and RT/ErGO/CPE when compared, it was observed that peak current for the oxidation of ABX enhanced five-times higher for RT/ErGO/CPE than that of nascent CPE (Fig. 2B). This is due to a synergistic effect between RT NPs and ErGO and well dispersion of RT NPs in the composite (Fig. S1).

### 3.3. Effect of accumulation time ($t_{acc}$) and potential ($E_{acc}$)

The effect of $t_{acc}$ was investigated at the open circuit in the range of 0–180 s (Fig. 3A) using cyclic voltammetric technique, wherein it was observed that peak current for the oxidation of ABX increased until 45 s and then decreased suddenly to remain unchanged beyond 60 s, due to the saturation of ABX concentration at the electrode surface. In addition, $E_{acc}$ was investigated in the range of +0.1 V–0.6 V. It was observed that $E_{acc}$ of +0.4 was optimum to get good results and hence, $t_{acc}$ 45 s and $E_{acc}$ of +0.4 were considered to be optimum for the present study.

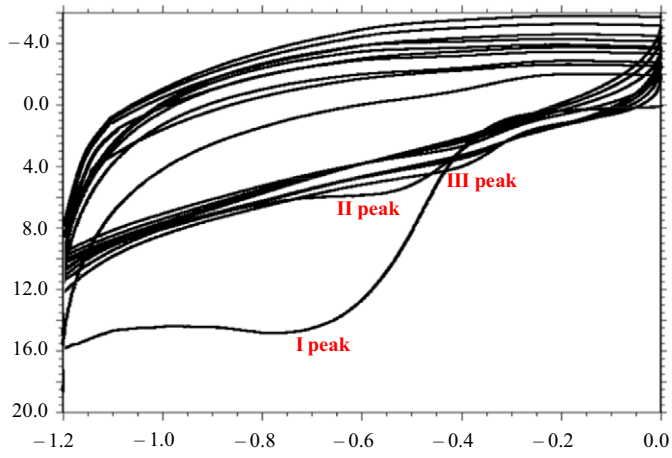


**Fig. 1.** Voltammogram for reduction of graphene oxide.

### 3.4. Influence of supporting electrolyte

The voltammograms for 0.01 mM ABX was recorded on the surface of RT/ErGO/CPE in an electrolyte solution of different pH from 3.0 to 11.2 (Fig. 3B) using the cyclic voltammetric technique. From Fig. 3C, showing a plot for the dependence of peak current on pH of the electrolyte solution, it was observed that buffer solution with pH 6.0 maximum peak current was obtained. Also, the peak potential had a more negative value as the pH increased (Fig. 3D). The fitted linear equation was:

$$E_p = -0.0518\ pH + 1.163; R^2 = 0.936 \quad (1)$$

When the slope obtained in the Eq. (1) was compared with the Nerst theoretical value (59.2 mV/pH), the slope was 51.8 mV/pH affirming that the electrode reaction takes place by transferring the same number of protons and electrons.

### 3.5. Effect of scan rate

Cyclic voltammograms were recorded for 0.01 mM ABX at the surface of RT/ErGO/CPE with different scan rate to understand the dependence of peak current and peak potential on scan rate (Fig. 4A). Scan rate and peak current of ABX oxidation were proportional to each other with a linear relationship (Fig. 4B) suggesting that adsorption-controlled process was predominant and the fitted equation was found to be as:

$$Ip = 288.5\ \upsilon + 16.05; R^2 = 0.990 \quad (2)$$

A linear plot for log υ vs. log Ip, the slope of 0.75 for RT/ErGO/CPE was close to the theoretical value of 1.0 for the electrode process to be called an adsorption-controlled process (Fig. 4C). The obtained linear equation was:

$$\log Ip = 0.75\ \log \upsilon + 2.395; R^2 = 0.993 \quad (3)$$

Further, the increasing scan rate moved peak potential for oxidation of ABX (Fig. 4D) to more of a positive value with the linear regression equation:

$$Ep = 0.057\ \log \upsilon + 1.038; R^2 = 0.996 \quad (4)$$

Laviron's equation was used to study the relationship between υ and Ep [49].

$$Ep = E^0 + \frac{2.303RT}{\alpha nF}\log\frac{RTk^0}{\alpha nF} + \frac{2.303RT}{\alpha nF}\log\upsilon \quad (5)$$

where Ep is peak potential, n is a number of electrons transferred, $k^0$ is the standard heterogeneous rate constant, α is the transfer coefficient, $E^0$ is the formal redox potential, $\nu$ is the scan rate and other terms have their standard meanings. The value of α was calculated as [50]:

$$\alpha = \frac{47.7}{Ep - E_{p/2}}\,mV \quad (6)$$

$E_{p/2}$ is the potential where the current is at exactly half of its peak value. αn was calculated as 1.03 for RT/ErGO/CPE and α was calculated to be 0.56 with electrons transferred calculated to be 1.8 ≈ 2.

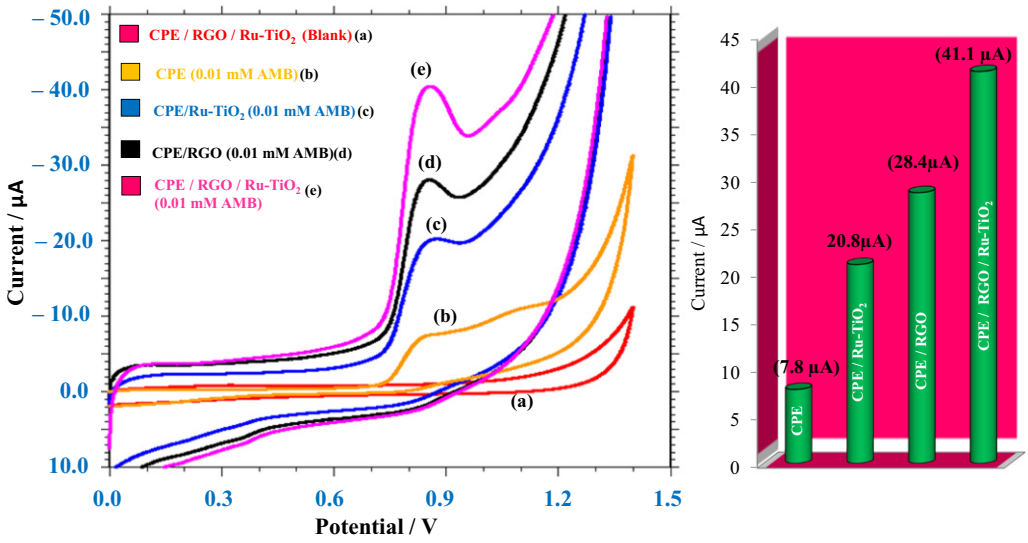


**Fig. 2.** Electrochemical behaviour of ABX; (A) voltammograms of 0.1 mM ABX (pH 6.0; Scan rate: 50 $mVs^{-1}$; $t_{acc} = 45$ s) (a)without ABX; (b) at CPE; (c) RT; (d) ErGo/CPE; (e) RT/ErGO/CPE; (B) Comparison of peak current of different electrodes.

### 3.6. Reaction mechanism

The results of scan rate variations were used to propose a probable electrochemical reaction of ABX on the surface of RT/ErGO/CPE with two protons and two electrons as in Scheme 1.

### 3.7. Analytical characteristics

Under optimum conditions mentioned above, a calibration graph was constructed to estimate ABX. Square wave voltammetric technique was recorded with an increasing concentration of ABX (Fig. 5A). In the linear range, the following equation was obtained (Fig. 5B):

$$I_p = 271.47\, C_{ABX} + 32.79; R^2 = 0.992 \quad (7)$$

Limit of detection (LOD) and quantification (LOQ) was calculated using the equations LOD = 3SD/m and LOQ = 10SD/m, where SD and m refer to standard deviation of blank and slope of calibration plot, respectively (Table 2). LOD and LOQ values were found to 1.05 nM and 3.53 nM for RT/ErGO/CPE. The LOD compared with the earlier reported data were lower (Table 1).

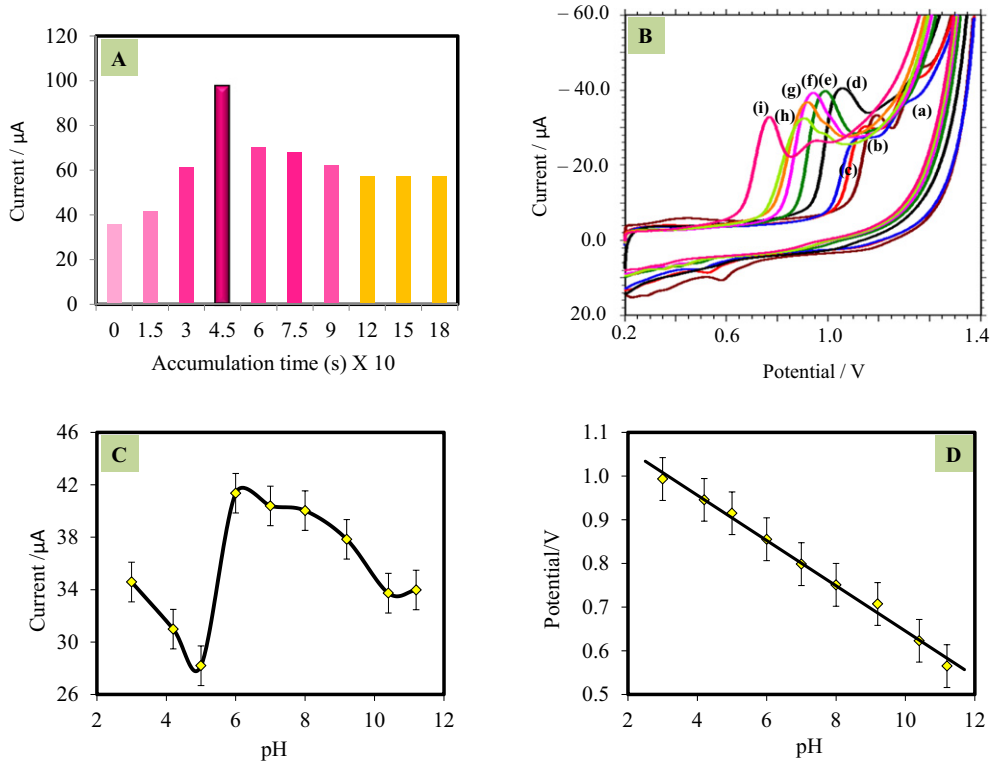


**Fig. 3.** (A) Accumulation time vs peak current; (B) voltammograms for 0.01 mM ABX on RT/ErGo/CPE recorded at: a) 3.0; b) 4.2; c) 5.0; d) 6.0; e) 7.0; f) 8.0; g) 9.2; h) 10.4 and i) 11.2 pH; (C) effect of pH on peak current ($I_p$); (D) effect of pH on peak potential ($E_p$).

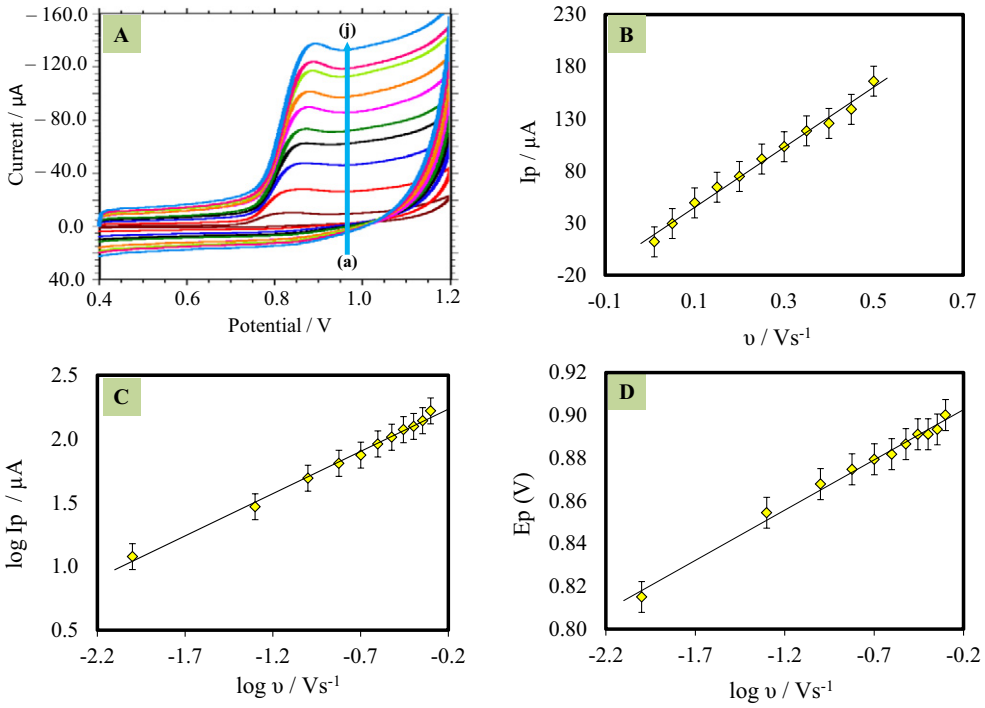


**Fig. 4.** (A) Cyclic voltammograms of 0.1 mM ABX on RT/ErGO/CPE at scan rate: (a) 10; (b) 50; (c) 100; (d) 150; (e) 200; (f) 250; (g) 300; (h) 350; (i) 400 and (j) 450 $mVs^{-1}$ at pH 6.0. (B) Peak current versus scan rate; (C) log peak current versus log scan rate; (D) peak potential versus log scan rate.

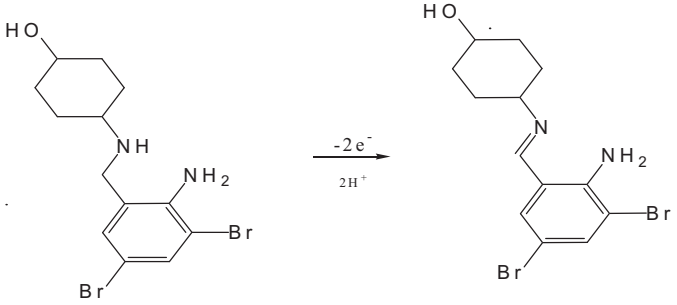


**Scheme 1.** Probable electrode reaction mechanism of ABX.

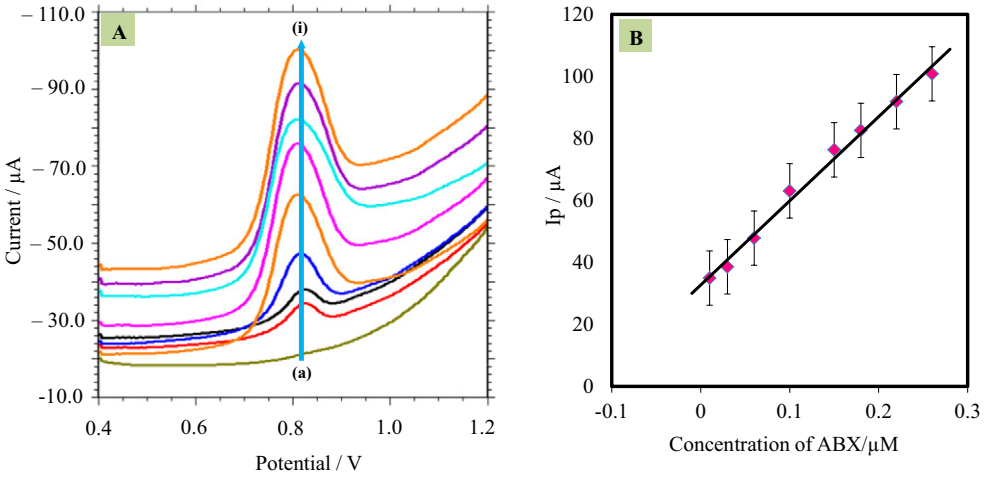


**Fig. 5.** (A) Square wave voltammogram for increasing concentration of ABX at ErGO/SDS/CPE; (a) 0.01; (b) 0.05; (c) 0.10; (d) 0.15; (e) 0.20; (f) 0.25; (g) 0.30; (h) 0.50 (i) 0.70 and (j) 1.0 µM; (B) concentration of ABX versus peak current.

**Table 1**
Comparison of detection limits of ABX with the earlier reported methods.

| Method | LOD (nM) | References |
|---|---|---|
| [a] | 50 | [51] |
| [b] | 1.0 | [15] |
| [c] | 940 | [52] |
| [d] | 10 | [53] |
| [e] | 1.05 | Present work |

[a] Stripping voltammeter; [b] multi-walled carbon nanotube/nafion-modified glassy carbon electrode; [c] glassy carbon electrode; [d] boron-doped diamond electrode; [e] RT/ErGO/CPE.

**Table 2**
Calibration plot characteristics of ABX studied using SWV.

| Characteristic | RT/ErGO/CPE |
|---|---|
| Linearity range (M) | $1.0 \times 10^{-5}$ to $1.0 \times 10^{-7}$ |
| Slope | 271.47 |
| Intercept | 32.72 |
| Correlation coefficient (r) | 0.9924 |
| Slope RSD (%) | 0.60 |
| Intercept RSD (%) | 0.20 |
| Number of data points | 8.0 |
| LOD (nM) | 1.05 |
| LOQ (nM) | 3.53 |
| Repeatability (RSD %) | 1.62 |
| Reproducibility (RSD %) | 2.60 |

### 3.8. Effect of excipients

Common excipients present in pharmaceutical drug formulation can affect the voltammetric signals during the analysis of dosage form. Hence, the selectivity of the electrode was investigated by studying the effect of common excipients present in (Fig. 6). The maximum concentration that gave less than ±5% error was considered as the tolerance limit. Common excipients such as lactose, glycine, urea, sucrose, gum acacia, starch, dextrose, citric acid, and oxalic acid were used for the investigation. The concentration of excipients used was 100-folds higher than that of ABX (0.1 mM). The results obtained showed no interference from any excipients. Hence, the studies suggested that RT/ErGO/CPE could be used for the determination of ABX in pharmaceutical and biological samples without significant interference from the commonly present interfering species.

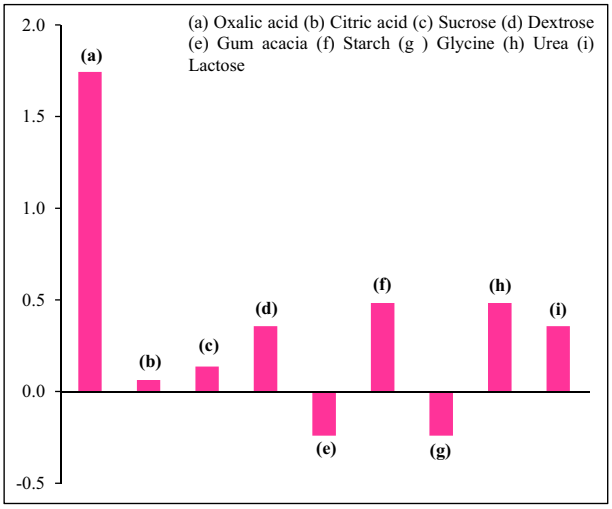


**Fig. 6.** Influence of potential interferents on the voltammetric response for ABX.

### 3.9. Tablet analysis

The developed electrode was applied for ABX determination in human urine samples as well as in pharmaceutical dosage forms. The investigations were performed by the standard addition method and recovery studies were performed using a square wave voltammetric technique (Table 3). Recovery values obtained from the tablet analysis were in the range of 94.8–100.6% for RT/ErGO/CPE. Good recoveries and good agreements between the manufacturer label and results obtained from the proposed method suggested that our sensor could be useful in the quality control.

### 3.10. Urine analysis

Drug-free samples were collected from five healthy volunteers, which were diluted a hundred-times and an appropriate clear supernatant solution was transferred to a 50 mL volumetric flask. A stock solution of ABX (1.0 mL) was then added to the flask and diluted up to the mark with a phosphate buffer solution (pH 6.0). The appropriate solution was transferred to a voltammetric cell to record the voltammograms. The results showed good recovery in the range of 97.8–101.7% with RSD of 1.5% for RT/ErGO/CPE, and hence, the proposed method can be applied for real sample analysis (Table 4).

### 3.11. Repeatability and reproducibility

The repeatability of the fabricated RT/ErGO/CPE was studied for 1.0 mM ABX for five replications. The same standard solution of ABX and the same electrode was used for the investigations. The relative standard deviation was calculated with % RSD value that was found to be 1.6% for RT/ErGO/CPE. In addition, the reproducibility of the electrode was investigated for five electrodes prepared from the same batch of electrode material for 1.0 mM ABX. The % RSD of 2.1% for RT/ErGO/CPE was observed. The results obtained were acceptable for RT/ErGO/CPE as a sensor for the determination of ABX. Further, the storage capability

**Table 3**
Tablet analysis.

| Characteristics | RT/ErGO/CPE |
|---|---|
| Label content | 100 mg |
| Amount recovered[a] | 98.2 mg |
| RSD (%) | 2.09 |
| $t_{tab}$ value[b] | 0.49 |
| $F_{tab}$ value[b] | 0.983 |
| Bias (%)[a] | −1.78 |
| Added (mg) | 100 |
| Found (mg)[a] | 96.56 |
| RSD (%)[a] | 2.62 |
| Bias (%)[a] | −1.5 |

[a] Average of five replicates.
[b] At 95% confidence level for four degrees of freedom.

**Table 4**
Analysis of ABX in spiked human urine samples by SWV and recovery studies.

| Spiked ($10^6$M) | Detected ($10^6$M) | Recovery (%)[a] | RSD %[a] |
|---|---|---|---|
| 0.4 | 0.389 | 97.2 | 1.08 |
| 0.6 | 0.599 | 99.8 | 1.05 |
| 0.8 | 0.786 | 98.2 | 1.07 |
| 1.0 | 0.987 | 98.7 | 1.06 |
| 2.0 | 1.948 | 97.4 | 1.07 |

[a] Average of five replicates.

of the electrode was investigated for five weeks and found to exhibit no significant changes in the detection level of ABX. The results were obtained with high recovery for pharmaceutical as well as urine samples, with low % of RSD values that demonstrated the repeatability, reproducibility, and stability of the electrode fabricated, suggesting its potential as a sensor for the determination of ABX in real sample analysis.

## 4. Conclusions

The proposed construction of a rapid and sensitive electrochemical sensor for the determination of ABX was quite effective. Reduced graphene oxide surface was easily converted to surface with a more active surface with the addition of RT to obtain much higher sensitivity. Thus modified electrode was having higher efficiency in the electrocatalytic oxidation of ABX as per the electrochemical investigations performed by the cyclic voltammetry in a phosphate buffer solution (pH 6). The results showed that RT/ErGO/CPE electrode showed a higher sensing ability than the nascent electrode. In addition, a square wave voltammetric technique was also developed for the determination of ABX but its limit of detection was much lower than those data repeated in the literature. Higher recoveries from pharmaceutical and human urine samples as well as the stability of the electrode suggested the direct application of the method developed for real sample analysis without the need for separation and complex solution. The proposed method was simple, easy to operate, has low cost and is time-saving, achieving a higher sensitivity than the earlier developed other methods.

Supplementary data to this article can be found online at https://doi.org/10.1016/j.molliq.2019.112368.

## Author statement

The authors listed in the manuscript have contributed in this research work, and agreed to submit the manuscript to this journal.

## Declaration of competing interest

The authors report no conflict of interest.

## References


[1] E. Houtmeyers, R. Gosselink, G. Gayan-Ramirez, et al., Eur. Respir. J. 14 (1999) 452–467.
[2] D.F. Rogers, Respir. Care 52 (2007) 1176–1197.
[3] D. Oliveri, G. Zavattini, G. Tomasini, et al., Respiration 51 (1987) 42–51.
[4] P.J. Poole, P.N. Black, BMJ 322 (2001) 1271–3 7.
[5] M. Malerba, A. Ponticiello, A. Radaeli, et al., Pulm. Pharmacol. Ther. 17 (2004) 27–34.
[6] G. Caramina, R. Gagliardini, E. Ruffi ni, et al., J Int Med Res 23 (1995) 284–293.
[7] G. Fegiz, Lung 169 (1991) 69–76.
[8] R.R. Wauer, G. Schmalisch, B. Böhme, et al., Eur. J. Pediatr. 151 (1992) 357–363.
[9] A. Gillissen, D. Nowak, Respir. Med. 92 (1998) 609–623.
[10] M.L. Qi, P. Wang, R.H. Cong, J.J. Yang, J. Pharmaceut. Biomed. 35 (2004) 1287–1291.
[11] G. Bazylak, L.J. Nagels, J. Pharmaceut. Biomed. 32 (2003) 887–903.
[12] H. Kim, J.Y. Yoo, H.J. Lee, K.R. Lee, J. Pharmaceut. Biomed. 32 (2003) 209–216.
[13] H. Dincer, N.G. Goger Basan, J. Pharmaceut. Biomed. 31 (2003) 867–872.
[14] L. Colombo, F. Marcucci, M.G. Marini, P. Pierfederici, E. Mussini, J. Chromatogr. Biomed. 530 (1990) 141–147.
[15] B.T. Demircigil, B. Uslu, Y. Ozkan, S.A. Ozkan, Z. Senturk, Electroanalysis 15 (2003) 230–234.
[16] V. Erady, R.J. Mascarenhas, A.K. Satpati, A.K. Bhakta, Z. Mekhalif, J. Delhalle, Microchem. J. 146 (2019) 73–82.
[17] S.D. Bukkitgar, N.P. Shetti, R.M. Kulkarni, S.D. Kulkarni, ECS J. Solid State Science and Technology 7 (2018) Q3215–Q3220.
[18] G. Manasa, R.J. Mascarenhas, B.M. Basavaraja, Colloids Surf. B: Biointerfaces 184 (2019), 110529.
[19] G. Manasa, A.K. Bhakta, Z. Mekhalif, R.J. Mascarenhas, Electroanalysis 31 (2019) 1363–1372.
[20] S.D. Bukkitgar, N.P. Shetti, Anal. Methods 9 (2017) 4387–4393.
[21] S.D. Bukkitgar, N.P. Shetti, R.M. Kulkarni, K.R. Reddy, S.S. Shukla, V.S. Saji, T. M Aminabhavi, J. Electrochem. Soc. 166 (9), B3072-B3078.
[22] F.S. Felix, C.M.A. Brett, L. Angnes, Talanta 76 (2008) 128–133.
[23] S. Salmanpour, A. Sadrnia, F. Karimi, N. Majani, V.K. Gupta, J. Mol. Liq. 254 (2018) 255–259.
[24] O.J. D'Souza, R.J. Mascarenhas, A.K. Satpati, B.M. Basavaraja, Science China Chem. 62 (2019) 262–270.
[25] M. Miraki, H.K. Maleh, M.A. Taher, S. Cheraghi, F. Karimi, S. Agarwal, V.K. Gupta, J. Mol. Liq. 278 (2019) 672–676.
[26] S. Ghosh, I. Calizo, D. Teweldebrhan, E.P. Pokatilov, D.L. Nika, A.A. Balandin, W. Bao, F. Miao, C.N. Lau, Appl. Phys. Lett. 92 (2008) 151911–151913.
[27] S. Kumar, S.D. Bukkitgar, S. Singh, V. Singh, K.R. Reddy, N.P. Shetti, C. Reddy, V. Sadhu, S. Naveen, ChemistrySelect 4 (2019) 5322–5337.
[28] C. Lee, X. Wei, J.W. Kysar, J. Hone, Science 321 (2008) 385–388.
[29] Y. Harima, S. Setodoi, I. Imae, K. Komaguchi, Y. Ooyama, J. Ohshita, H. Mizota, J. Yano, Electrochim. Acta 56 (2011) 5363–5368.
[30] R.R. Nair, P. Blake, A.N. Geim, Science 320 (2008) 1308.
[31] K.I. Bolotin, K.J. Sikes, Z. Jiang, M. Klima, G. Fudenberg, J. Hone, P. Kim, H.L. Stormer, Solid State Commun. 146 (2008) 351–355.
[32] D.A.C. Brownson, D.K. Kampouris, C.E. Banks, J. Power Sources 196 (2011) 4873–4885.
[33] P.S. Patil, Mater. Chem. Phys. 59 (1999) 185–273.
[34] N.P. Shetti, S.D. Bukkitgar, R.R. Kakarla, C. Reddy, T.M. Aminabhavi, Biosens. Bioelectron. 141 (2019), 111417.
[35] C.G. Granqvist, Sol. Energy Mater. Sol. Cells 91 (2007) 1529–1598.
[36] K.L. Chopra, S. Major, D.K. Pandya, Thin Solid Films 102 (1983) 1–5.
[37] M. Anpo, S. Dohshi, M. Kitano, Y. Hu, M. Takeuchi, M. Matsuoka, Annu. Rev. Mater. Res. 35 (2005) 1–27.
[38] N.P. Shetti, S.D. Bukkitgar, K.R. Reddy, C.V. Reddy, T.M. Aminabhavi, Colloids Surf. B: Biointerfaces 178 (2019) 385–394.
[39] H. Hao, J. Zhang, Micropor. Mesopor. Mater. 121 (2009) 52–57.
[40] N.R. Elezovic, B.M. Babic, V.R. Radmilovic, L.M. Vracar, N.V. Krstajic, Appl. Catal. B Environ. 140-141 (2013) 206–212.
[41] S. Shin, K. Kim, J. Choi, Electrochem. Commun. 36 (2013) 88–91.
[42] T. Ohno, F. Tanigawa, K. Fujihara, S. Izumi, M. Matsumura, J. Photoch. Photobio. A 127 (1999) 107–110.
[43] K.T. Ranjit, T.K. Varadarajan, B. Viswanathan, J. Photoch. Photobio. A 89 (1995) 67–68.
[44] G.D. Christian, W.C. Purdy, J. Electroanal. Chem. 3 (1962) 363–367.
[45] S.D. Bukkitgar, N.P. Shetti, R.M. Kulkarni, M.R. Doddamani, J. Electroanal. Chem. 762 (2016) 37–42.
[46] S.D. Bukkitgar, N.P. Shetti, Mater. Sci. Eng. C 65 (2016) 262–268.
[47] N.P. Shetti, S.J. Malode, D.S. Nayak, S.D. Bukkitgar, G.B. Bagihalli, R.M. Kulkarni, K.R. Reddy, J. Phys. Chem. Solids137, 109210.
[48] N.P. Shetti, D.S. Nayak, S.J. Malode, R.R. Kakarla, S.S. Shukla, T.M. Aminabhavi, Anal. Chim. Acta 1051 (2019) 58–72.
[49] E. Laviron, J. Electroanal. Chem. 101 (1979) 19–29.
[50] A.J. Bard, L.R. Faulkner, Electrochemical Methods Fundamentals and Applications, Second Ed Wiley, New York, 2004.
[51] I.H.I. Habib, S.I.M. Zayed, Pharmazie 60 (2005) 193–196.
[52] Y. Plao, Int. J. Electrochem. Sci. 7 (2012) 6084–6096.
[53] A. Leventa, Y. Yardımb, Z. Senturk, Sensors Actuators B 203 (2014) 517–526.